# Gaseous Fission Reactors for Booster Propulsion

ROBERT V. MEGHREBLIAN

Jet Propulsion Laboratory
Pasadena, Calif.

**The gaseous fission reactor concept is examined as the prime energy source for direct heating of the propellant in a high thrust rocket engine. The analysis reveals that, if regenerative cooling is the only mechanism for removing the radiation heat deposited in the solid members of the reactor and engine, the maximum attainable specific impulse is about three times that for the corresponding all solid fuel reactor. In the high thrust application, i.e., booster stages, thermal radiation from the fissioning gas is not a critical factor. Even with conservative estimates of gas emissivities, the resulting engine performance is markedly superior to other methods of propulsion. Typical engine and vehicle characteristics are determined for a variety of missions ranging from 25,000 to 60,000 fps velocity increments.**

THE PURPOSE of this paper is to examine the application of the gaseous fission reactor concept to the propulsion of ground takeoff rocket vehicles. Therefore, attention is focused on rocket engines capable of generating thrusts equal at least to their own weight.

The analysis is carried out with the aid of an ideal reactor model that incorporates a nuclear fuel-bearing region in the core which is *nontemperature-limited*. As noted in Ref. 1, this implies that, within a certain region of the core, the fuel-bearing material is in gas phase; it becomes possible, therefore, to let the temperature in this region exceed the allowable limits of the surrounding solid structural members of the engine. If this very hot, fissionable material is allowed to mix intimately with a propellant gas, then it becomes possible to heat the propellant to temperatures significantly greater than the temperature limits of the material of the containing structure, and substantial gains in specific impulse can be achieved.

It is not within the scope of this study to explore the problems associated with the gas phase heating and separation of a fissionable material and a propellant; these problems have been examined elsewhere (see, for example, Ref. 2). In the present work it is postulated that the desired effects can be obtained, and attention is directed to the overall implications of the gaseous reactor concept in terms of performance potential and operational constraints. Thus, the results obtained here are generally applicable to any gaseous reactor concept based on the idea of direct heating of a gaseous propellant by the slowing down of fission fragments. As already noted, such systems require intimate mixing of the fuel and propellant. These results do not apply directly, therefore, to such schemes as the gaseous core reactor using magnetic containment (3)[1] or the coaxial flow reactor (4), because, in these systems, the heat transfer from the nuclear fuel to the propellant is achieved principally by thermal radiation. Although some gross interpretations for such systems are possible, a reformulation of the problem would be required in order to obtain detailed characteristics (5).

When the gaseous reactor is used in the high thrust application, it is not feasible to incorporate a radiator in the engine complex. It has been shown that, although the inclusion of a radiator increases markedly the specific impulse attainable, the penalty in engine thrust to weight ratio is excessive, and the resulting system becomes incapable of ground takeoff (1). Thus, the engines considered here consist simply of reactor plus nozzle, and all cooling of the engine's solid components is achieved by a regenerative process with the aid of the propellant itself. The analysis does incorporate, however, the effect on the overall power balance in the system arising from the nuclear radiation produced by the fission process and the thermal radiation emitted by the very hot propellant gas in the cavities. Both phenomena produce a heat load on the engine solids which must be absorbed by the regenerative cooling action.

## Engine Characteristics

Fig. 1 shows a schematic of the proposed cavity reactor concept appropriate to the propulsion application. The nontemperature-limited fuel-bearing region, shown arbitrarily to occupy a central location in the core, contains the high temperature gas cavities that provide the propellant with the final heat input which raises it to the *chamber*, i.e., pre-rocket nozzle, temperature $T_c$. The temperature-limited region, shown in an annular location, operates at temperature $T_s < T_c$.

The power balance in the system is established on the basis that the propellant is first heated from the storage condition (say enthalpy per unit mass of propellant $h_0 = 0$) to the maximum solid temperature $T_s$, or corresponding enthalpy $h_s$, by first passing through the solid regions of the reactor which require cooling. The propellant is then introduced into the gaseous region, i.e., cavities, where the enthalpy is increased to $h$ corresponding to the chamber or cavity temperature $T_c$. Clearly, the total fission power $P$ produced in the reactor must be carried off by the propellant as kinetic energy. If $\dot{m}$ is the mass flow rate of propellant, then

$$P = \dot{m}h_c \qquad [1]$$

For reasons that will become apparent from the nuclear analysis, it may not be desirable to contain all of the fissionable material in gas phase, but rather to allow a certain fraction to be carried in, say, solid form. If $f$ denotes the fraction of the total fission power released in the solid fuel regions, then

---

R. V. MEGHREBLIAN, Member ARS, is Chief, Physical Sciences Division. Manuscript received Aug. 14, 1961. This article presents the results of one phase of research carried out at the Jet Propulsion Laboratory under Contract NASw-6, sponsored by NASA.

[1] Numbers in parentheses indicate References at end of paper.

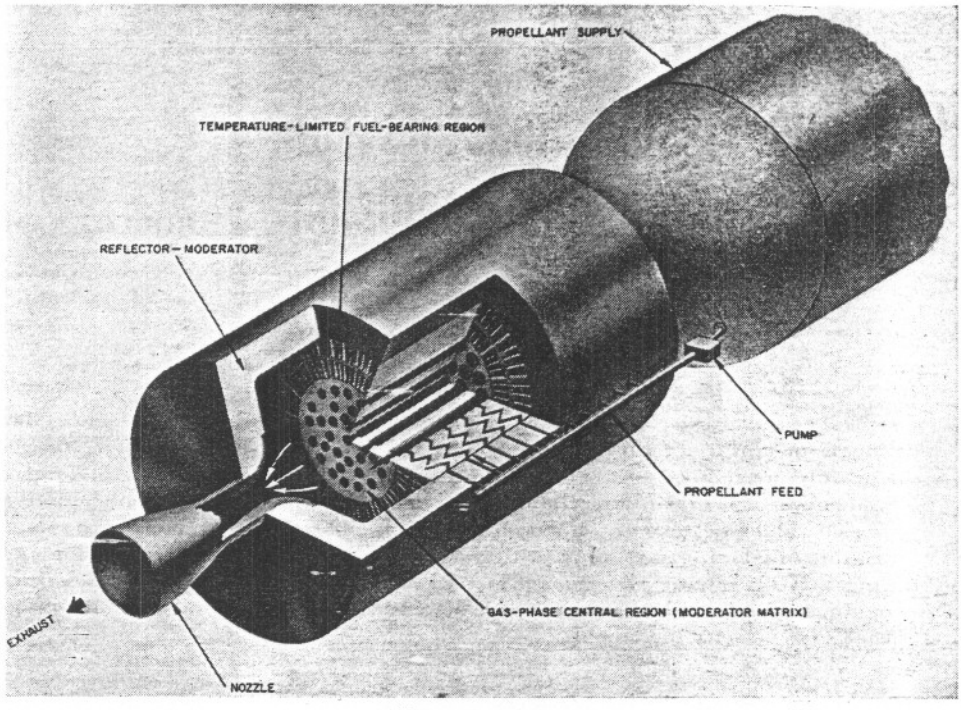


Fig. 1 Vortex cavity reactor schematic

the fraction released in the cavities is $(1 - f)$; however, the total power deposited in the solid region $P_s$ must also include the portion arising from the nuclear and thermal radiation emitted by the gaseous fuel. This may be written

$$P_s = fP + \zeta(1 - f)P + P_{rg} \qquad [2]$$

where $\zeta$ denotes the fraction of fission energy which appears in the form of nuclear radiation (i.e., gamma rays, and also partially from fast neutrons slowing down) that is attenuated principally by the solid regions in the engine, and $P_{rg}$ is the thermal power radiated by the hot cavity gases to the solid walls. If regenerative cooling by the propellant is the only mechanism for removing the heat attenuated in the solid, then

$$P_s = \dot{m}h_s \qquad [3]$$

The quantity $P_s$ may be eliminated between Eqs. 2 and 3, and by also using Eq. 1, the enthalpy ratio is obtained

$$\frac{h_c}{h_s} = \left(\mu + \frac{P_{rg}}{P}\right)^{-1} \qquad [4]$$

where $\mu$ is the fraction of the total fission power appearing directly in the solid regions

$$\mu \equiv f + \zeta(1 - f) \qquad [5]$$

The radiative power term may be written

$$\frac{P_{rg}}{\dot{m}h_s} = \beta\left(\frac{T_c^4}{T_s^4} - 1\right) \quad \beta \equiv \frac{\sigma\epsilon_c A_c T_s^4}{\dot{m}h_s} \qquad [6]$$

These relations imply that the gas mixture in the cavities is transparent and emits radiation at its central temperature $T_c$ as a gray body with emissivity $\epsilon_c$. The choice of a transparent gas for this analysis is somewhat arbitrary. There is reason to expect that for some combinations of fuel and propellant over certain temperature ranges, the mixture may very well be opaque. This question about the detailed radiative characteristics of the gas has been examined more carefully elsewhere (6). Analyses indicate that the choice between an opaque and transparent gas mixture for the high thrust gaseous reactor application is not critical, and either one will give a reasonable estimate of the thermal radiation heat load on the solid; for simplicity, the transparent gas is selected here.

A further approximation is introduced in selecting a temperature-enthalpy relation. Again, the simplest form is used, namely, $T_c/T_s = h_c/h_s$. (A more realistic relation has been shown (6) to be $T_c/T_s = (h_c/h_s)^{2/3}$.) Use of this linear form in Eqs. 6 and 4 yields

$$\left(\frac{I_c}{I_s}\right)^2 = \frac{1}{\mu}\left\{1 - \beta\left[\left(\frac{I_c}{I_s}\right)^8 - 1\right]\right\} \qquad [7]$$

where the familiar relation $I_i = \sqrt{2h_i/g}$, the specific impulse for a completely expanded de Laval nozzle starting with stagnation enthalpy $h_i$, has been used. The solutions for $I \equiv I_c/I_s$ from Eq. 7 are shown in Fig. 2 as a function of the thermal radiation parameter $\beta$ for various values of the fission

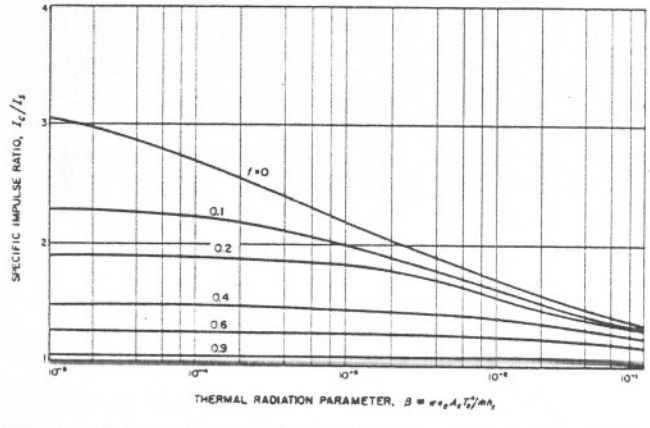


Fig. 2 Specific impulse ratio as function of thermal radiation parameter

fraction $f$. It is seen that substantial gains in specific impulse are achieved principally at the smaller values of $\beta$, i.e., at low values of the emissivity of the propellant in the cavities, and at the smaller values of the fission fraction, i.e., most of the fission power must be released in the gas phase. The significance of these results in terms of system performance potential have been discussed in Ref. 1. The essential observation to be made here is that the specific impulse varies inversely as the nuclear radiation parameter $\zeta$. The effect of the fission fraction $f$ and the thermal radiation parameter $\beta$ is to increase the effective value of $\zeta$, with the result that the maximum attainable specific impulse is reduced. The most important conclusion to be drawn is that there is, for a completely regeneratively cooled engine, a maximum specific impulse ratio possible even in the reactor with a nontemperature-limited fuel-bearing region. The limit occurs when $\beta = f = 0$, and is simply $I_{max} = \zeta^{-1/2}$. In terms of a reasonable set of reactor parameters, for example, $I_s = 700$ sec (which corresponds to a hydrogen propellant at $T_s = 2000°K$), this yields $I_c = 2210$ sec.

The manner in which the total power produced in the reactor is transferred to the propellant is a very sensitive function of the thermal radiation parameter and the fission fraction. Fig. 3 shows the distribution between the regenerative cooling process and the cavity region heating for some representative cases. It is to be noted that the total power lost to the regenerative process becomes significant for values of $\beta > 10^{-3}$. The portion of the heat load in the solid due to thermal radiation becomes significant, however, when $\beta$ exceeds about $10^{-2}$. Fig. 4 shows a plot of the maximum value of the fission fraction, as a function of the thermal radiation parameter, at which the thermal radiation exceeds the nuclear. For a given value of $\beta$, values of $f$ less than those indicated result in thermal radiation heat loads greater than those of the nuclear, and for values of $f$ greater than indicated, less than those of the nuclear.

The two parameters $f$ and $\beta$ determine not only the specific impulse of the engine, but the thrust to weight ratio as well. For the purpose of this analysis, this dependency is adequately established by selecting a simplified model of the engine which consists only of the reactor. It is convenient to define the reactor weight $W_n$ in terms of a maximum permissible power density $p_s$ in the solid regions of the reactor. Then, if $w_s$ is the weight per unit volume of the solid, the reactor weight is given by

$$W_n = \frac{w_s P_s}{p_s} \qquad [8]$$

As previously argued (1), the choice of this parameter is intended only to simplify the analysis and should not necessarily be considered the best means of defining the reactor size.

Eq. 8 may be used to compute the engine thrust to weight ratio. If $F$ is the rocket engine thrust, then $F = \dot{m}c_e$, and it follows from Eqs. 8 and 3 that

$$\frac{F}{W_n} = I\theta \qquad [9]$$

with $\theta = 2p_s/w_s c_s$ and $c_s = I_s g$, the exhaust velocity for a rocket motor having stagnation enthalpy $h_s$. It is to be noted that $\theta$ is simply the thrust to weight ratio for an all solid fuel reactor with exhaust velocity $c_s$. Thus, as $I$ exceeds unity through the use of gas phase heating, $F/W_n$ is improved over that possible in an all solid fuel reactor.

Given the power density $p_s$, $w_s$, and $c_s$, the total reactor power and hence size are directly established. Consider first the total power: it follows from Eq. 1 and the relation for the thrust $F$ that

$$P = \frac{FIc_s}{2} \qquad [10]$$

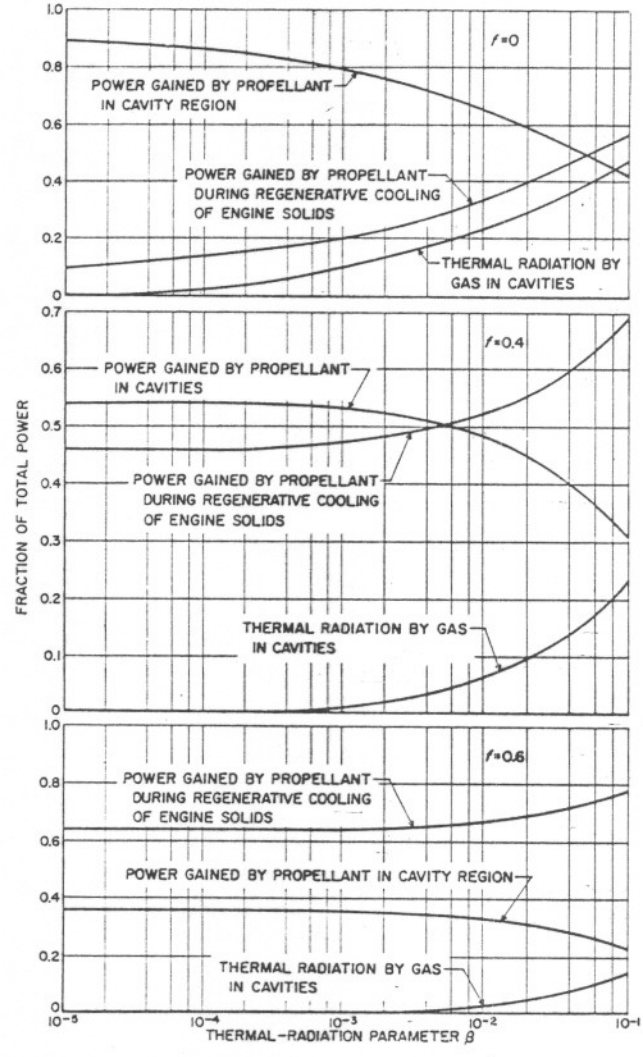


**Fig. 3 Power distribution in engine without radiator**

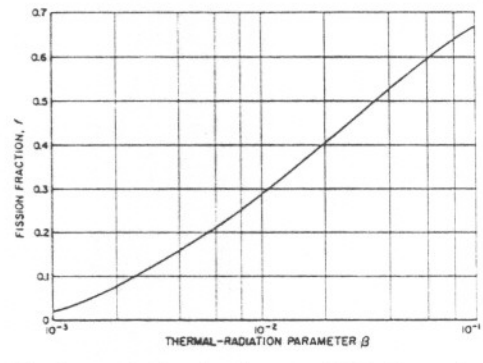


**Fig. 4 Maximum fission fraction at which thermal radiation exceeds nuclear radiation**

The total power deposited in the solid $P_s$ is then easily shown to be

$$\frac{P_s}{P} = \frac{1}{I^2} \qquad [11]$$

From this result, the reactor volume $V_n$ is obtained directly. If $x$ is the void fraction occupied by the gaseous fuel contain-

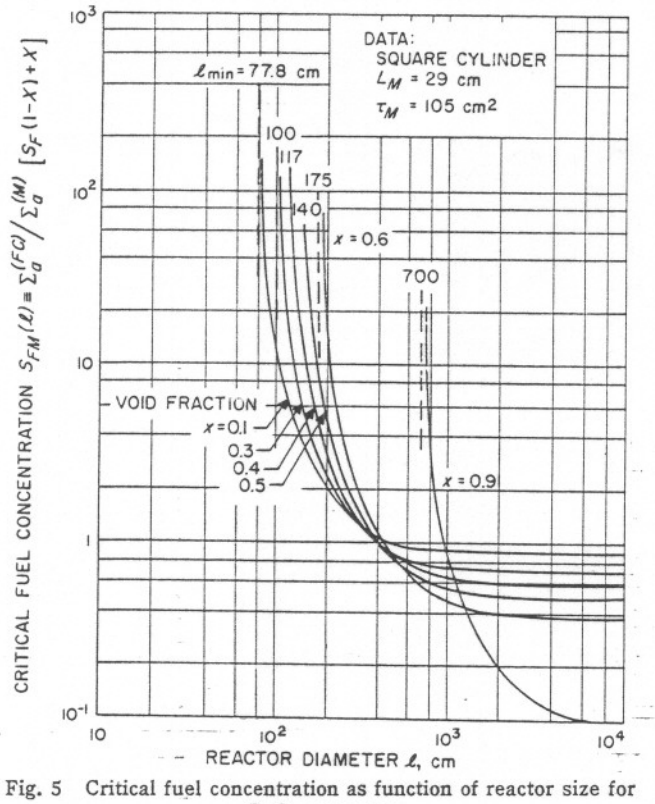


Fig. 5 Critical fuel concentration as function of reactor size for BeO moderator

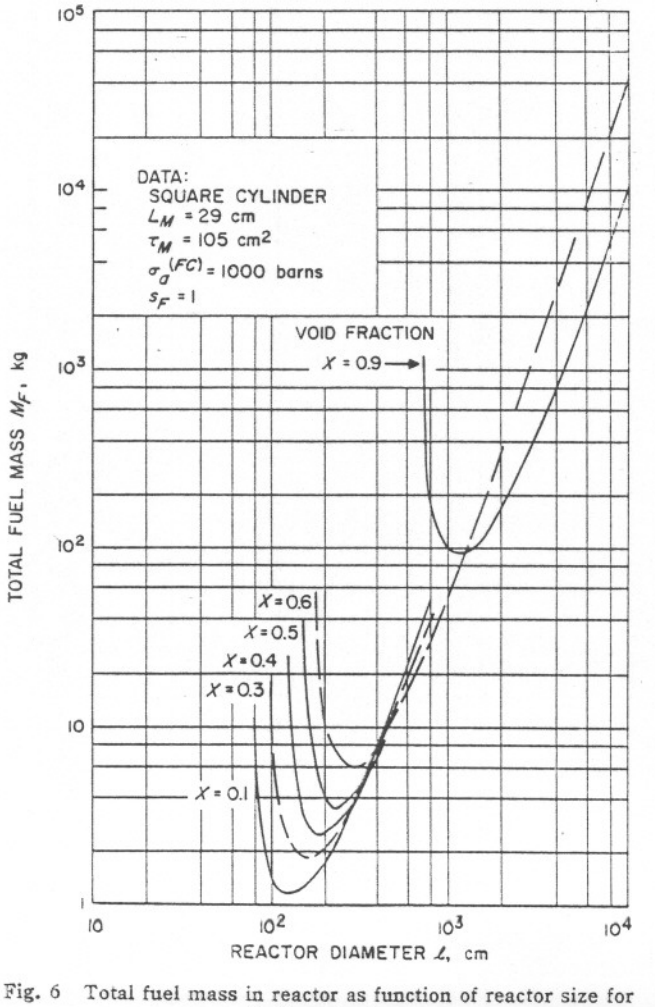


Fig. 6 Total fuel mass in reactor as function of reactor size for BeO moderator

ing cavities in the reactor, then, using Eq. 10

$$V_n = \frac{c_s F}{2p_s(1-x)I} = \frac{P}{p_s(1-x)I^2} \qquad [12]$$

This yields, for the length $l$ of a cylindrical reactor with diameter equal to length

$$l = \left[\frac{4'}{\pi I(1-x)}\left(\frac{F}{w_s\theta}\right)\right]^{1/3} \qquad [13]$$

It is seen that, given the various engine parameters, the vehicle payload and mission requirements determine $F$, and thence $l$.

## Reactor Characteristics

Once the reactor size is determined from the total power, or thrust, and engine parameters, calculating the nuclear characteristics of the reactor is a straightforward task. Again, it is appropriate to select an elementary model for this purpose to simplify the analysis. On this basis, the Fermi age theory is selected, with the expectation that it will give reasonable estimates of the essential features, namely, the critical fuel mass and average thermal neutron flux. The computation is further simplified by assuming a homogeneous bare reactor; a gross volume correction is applied to the various nuclear parameters to account for the presence of the cavities.

If the product of the fast effect and the resonance escape probability to thermal is taken as unity, then the usual criticality relation may be written

$$\frac{\eta f_* \exp(-B^2\bar{\tau})}{1 + L^2B^2} = 1 \qquad [14]$$

where $f^*$ is the thermal utilization. $L$ the diffusion length, $B$ the buckling, and $\tau$ the age to thermal. On the basis of the model specified above, these are given by

$$f_* = \frac{\bar{\Sigma}_a^{(F)}}{\bar{\Sigma}_a^{(F)} + \bar{\Sigma}_a^{(M)}} \qquad [15a]$$

$$L^2 = \frac{1}{3\Sigma_{tr}[\bar{\Sigma}_a^{(F)} + \bar{\Sigma}_a^{(M)}]} \qquad [15b]$$

where

$$\bar{\Sigma}_a^{(F)} = \Sigma_a^{(FC)}[S_F(1-x) + x]$$

$$\bar{\tau} \simeq \frac{\tau_M}{(1-x)^2} \qquad \Sigma_{tr} \simeq \Sigma_{tr}^{(M)}(1-x) \qquad D \simeq \frac{D_M}{1-x} \qquad [16]$$

and

$$S_F = \frac{\Sigma_a^{(FS)}}{\Sigma_a^{(FC)}} \qquad [17a]$$

$$s_F = \frac{\sigma_a^{(FS)}}{\sigma_a^{(FC)}} \qquad [17b]$$

The symbol $\Sigma_a^{(FS)}$ denotes the actual macroscopic absorption cross section of the fuel in the solid region and $\Sigma_a^{(FC)}$ that in the cavity region; $(\ )_M$ refers to the pure moderator material, and the remaining symbols have the usual definitions given in reactor theory (7). With these relations, the critical Eq. 14 may be solved for the macroscopic absorption cross section of the fuel in the cavity regions

$$S_{FM} = \frac{\Sigma_a^{(FC)}}{\Sigma_a^{(M)}}[S_F(1-x) + x]$$

$$= \frac{(1-x)^2 + B^2L_M^2}{(1-x)\{\eta \exp[-B^2\tau_M(1-x)^{-2}] - 1\}} \qquad [18]$$

The function $S_{FM}(l)$ is shown in Fig. 5 for $Pu^{239}$ fuel and BeO moderator at several values of the void fraction. The singularities correspond to the minimum reactor size at which a BeO moderator can support a self-sustaining chain reaction. The minimum size reactors are given by

$$l_{\min} = \frac{1}{1 - x}\left[\frac{\tau_M(\pi^2 + 4\nu_1^2)}{\ln \eta}\right]^{1/2} \qquad [19]$$

The symbol $\nu_1$ denotes the first zero of the zeroth-order Bessel function. The horizontal asymptotes correspond to infinite multiplying media and yield the minimum fuel concentrations

$$S_{FM}(\infty) = \frac{1 - x}{\eta - 1} \qquad [20]$$

The result (Eq. 18) may also be used to compute the fuel concentration $N_{FS}$ in the solid region of the reactor; thus, with $N_{FC}$ denoting the fuel concentration in the cavity region

$$N_{FS} = \frac{S_F}{s_F} N_{FC} \qquad [21]$$

The average fuel concentration $N_F$ for the whole reactor is given by

$$N_F = N_{FC}\left[x + (1 - x)\frac{S_F}{s_F}\right] \qquad [22]$$

The total critical fuel mass $M_F$ is obtained from the above results. This quantity may be written

$$M_F(l) = \frac{A_F}{\mathcal{A}}\left[x + (1 - x)\frac{S_F}{s_F}\right] N_{FC}(l) V_n(l) \qquad [23]$$

where $A_F$ is the molecular weight of the fuel material and $\mathcal{A}$ Avogadro's number. In the event that the same nuclear fuel is used in both the solid and gas phase, $s_F = 1$, and Eq. 23 reduces to

$$M_F(l) = \frac{A_F \Sigma_a^{(M)} V_n(l) S_{FM}(l)}{\mathcal{A}\sigma_a^{(FC)}} \qquad [24]$$

This result is plotted in Fig. 6. The minimum critical mass and corresponding reactor diameters are shown in Fig. 7 as a function of the void fraction. It is seen that, for reasonable void fractions ($0.3 < x < 0.6$), the total fuel investment ranges from 2 to 6 kg, with reactor diameters of from 200 to 300 cm. The corresponding reactor weights vary from about 20,000 to 100,000 lb. With so large an investment in reactor weight, it is to be expected that these systems will be most suitable for missions involving the acceleration of very large payloads through rather large velocity increments.

The average thermal neutron flux in the reactor is determined from the total power output. If $\epsilon$ is the energy release per fission reaction, then

$$P = \epsilon V_n \Sigma_f^{(FC)} \phi_c[\alpha(1 - x) + x] \qquad [25]$$

where the fuel distribution parameter $\alpha$ is defined

$$\alpha \equiv \frac{\Sigma_f^{(FS)}\phi_s}{\Sigma_f^{(FC)}\phi_c} = S_F\left(\frac{\phi_s}{\phi_c}\right)\left(\frac{1 + \alpha_c}{1 + \alpha_s}\right) \qquad [26]$$

The symbol $\alpha_i$ denotes the ratio of the radiative capture to fission cross section of the fuel in region $i$; $\phi_s$ is the average thermal flux in the solid region of the reactor, and $\phi_c$ that in the cavity region. The parameter $\alpha$ is related to the fission fraction $f$ through the equation

$$f = \frac{\alpha(1 - x)}{\alpha(1 - x) + x} \qquad [27]$$

If the average power density $P/V_n$ is eliminated with the aid of Eq. 12, then $\phi_c$ may be obtained from Eq. 25; thus

$$\phi_c = \frac{p_s(1 - x)(1 + \alpha_c)I^2}{\epsilon\Sigma_a^{(FC)}[\alpha(1 - x) + x]} \qquad [28]$$

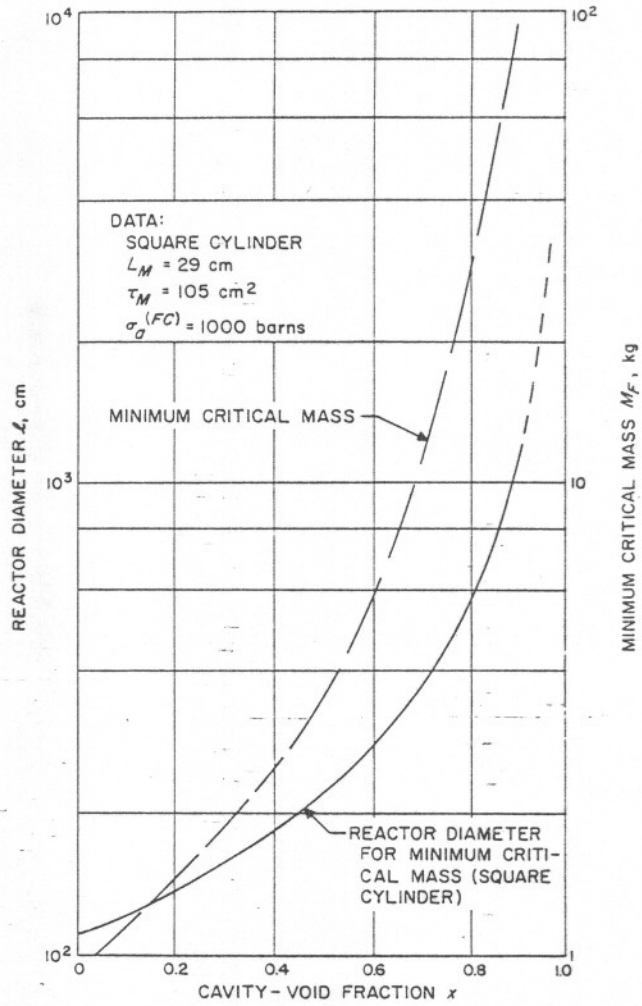


**Fig. 7 Optimum characteristics of BeO moderated reactor as function of void fraction**

## Vehicle Performance

Some indication of the performance capabilities of rocket vehicles propelled by fission reactors using gas phase heating may be obtained from simple burnout-velocity calculations based on a drag-free vertical trajectory. In the case of a single-stage vehicle, the burnout velocity is given by the well-known relation

$$V = -I \ln\left(1 - \frac{W_p}{W_0}\right) - \frac{IW_p}{a_0 W_0} \qquad [29]$$

where $W_p$ is the propellant weight, $W_0$ the initial gross weight, $a_0$ the initial acceleration in units of the gravitational constant, and $V$ the ratio of the velocity increment, acquired during acceleration, to the quantity $c_s$. The specification of the mission is complete upon the selection of the payload weight $W_{pl}$ to be delivered. For the present systems this is related to the gross weight by

$$\pi_{pl} = \frac{W_{pl}}{W_0} = 1 - \frac{W_p}{W_0}(1 + s) - \frac{a_0}{\theta I}$$

where $s$ is the ratio of the propellant tank weight to the weight

of the propellant. Thus the vehicles considered here consist simply of payload, propellant plus tanks, and reactor (accounted for by the last term in the above expression).

Calculations based on these relations have been carried out for a variety of missions, beginning with an Earth-satellite launch, $V = 1.14$, and extending to $V = 2.5$. Generalized results for the payload fraction as a function of the thermal radiation parameter for various values of the fission fraction are given in Fig. 8. These results are based on the following values of the parameters involved: $\zeta = 0.1$, $s = 0.05$, $a_0 = 1.3$, and $\theta = 20$. The value for $\theta$ corresponds to a reactor with an average density $w_s = 3$ gm/cm³, $c_s = 22{,}400$ fps, and a power density $p_s = 2$ kw/cm³, a fairly representative set for present day power reactor technology. These curves, along with the analytical results for $P$, $l$, and the information in Fig. 5, should be helpful in estimating the vehicle and engine characteristics, given the dimensionless velocity increment $V$ and the payload to be delivered. As may be noted from Fig. 8, the most effective use of the system in a single-stage configuration is in the Earth-satellite and escape missions. Higher performance missions such as $V = 2$ and 2.5, although possible with not insignificant payload fractions, result in increasingly larger total launch weights. For these applications, the single-stage system is not the most attractive, and, as with chemical engines, substantial gains in payload fraction may be achieved by introducing additional powered stages, nuclear or otherwise. It is interesting to note, however, that for the satellite mission in particular the payload represents some 20 to 40% of the launch weight when the gas phase heating provides 60% or more of the total energy transferred to the propellant. These systems appear especially well suited as Earth to satellite orbit freight vehicles. The single stage, possibly coupled with a recoverable engine, would very likely yield an economical and efficient technique for placing large payloads, such as low acceleration spacecraft, into orbit in preparation for interplanetary missions.

Specific systems computations carried out for the Earth-satellite mission indicate the magnitude of the principal vehicle and engine characteristics to be expected for such applications. Fig. 9 shows the vehicle gross weight at launch, the reactor weight, power, and diameter, and the specific im-

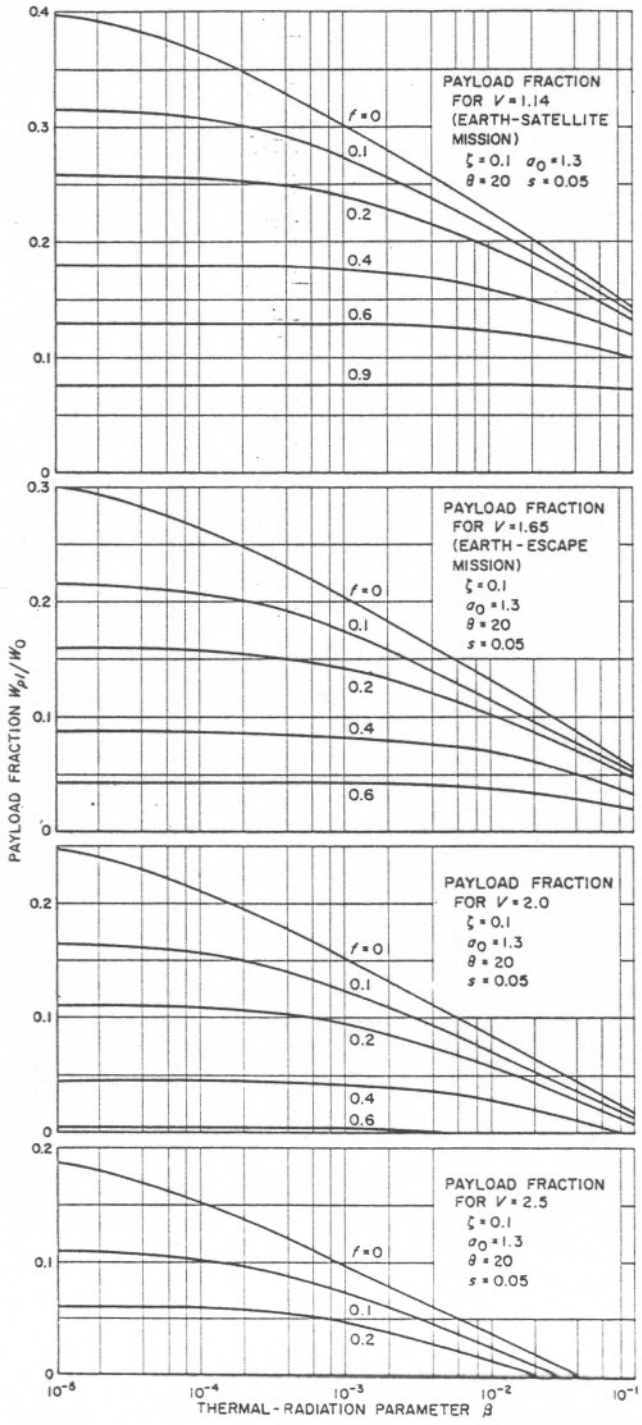


Fig. 8 Payload fraction as function of thermal radiation parameter for various values of fission fraction

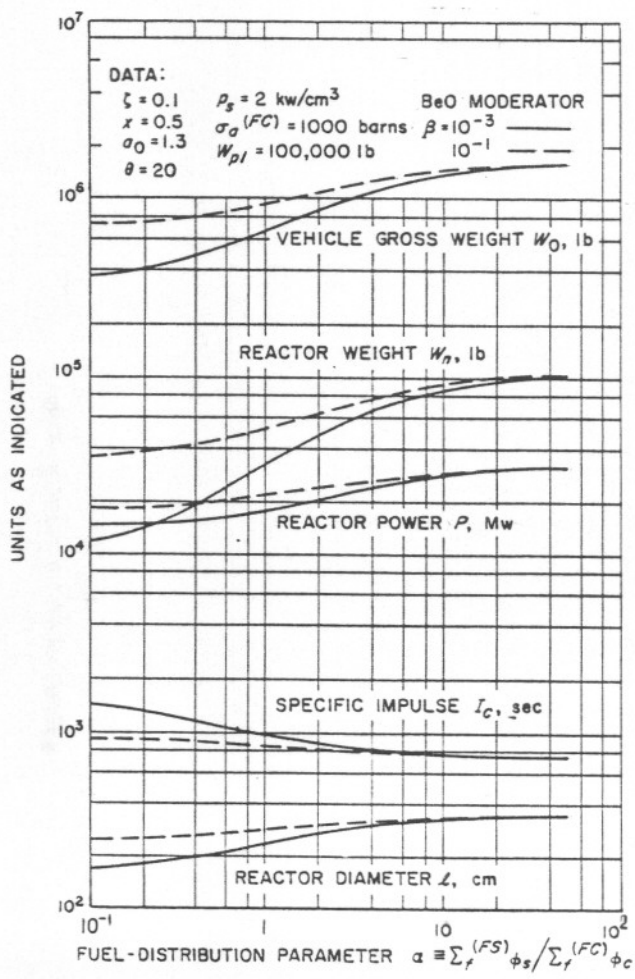


Fig. 9 Vehicle and engine characteristics as function of fuel-distribution parameter for Earth-satellite mission

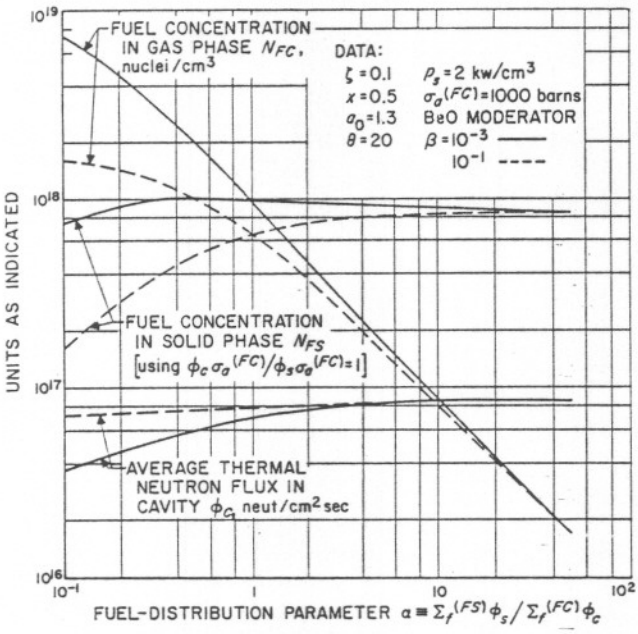


Fig. 10 Fuel concentration and average thermal flux as function of fuel-distribution parameter for Earth-satellite mission

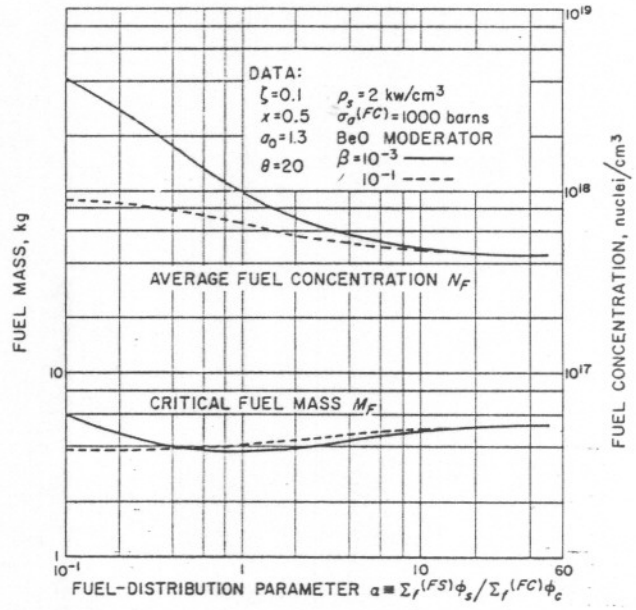


Fig. 11 Average fuel concentration and critical mass as function of fuel-distribution parameter for Earth-satellite mission

pulse for a vehicle to place a 100,000-lb payload in Earth-satellite orbit. These data are plotted as a function of the fuel distribution parameter $\alpha$ for two values of the thermal radiation parameter, $\beta = 10^{-3}$ and $10^{-1}$. The engine parameters used for these computations are $\zeta = 0.1$, $x = 0.5$, $a_0 = 1.3$, $\theta = 20$, $p_s = 2$ kw/cm³, and $\sigma_a^{(FC)} = 1000$ barns; BeO moderator was selected for the reactor. It is interesting to note that at the higher values of $\alpha$ the system characteristics become somewhat insensitive to $\beta$. This is to be expected, since large values of $\alpha$ imply that the bulk of the fuel is carried in the solid regions of the reactor. Consequently, the thermal radiation from the propellant in the cavities becomes an increasingly smaller portion of the total heat load in the solid regions, and the emissivity of this hot gas has less influence on the system. This behavior is most clearly revealed by the effect of $\alpha$ on the specific impulse. As larger fractions of the fission energy are released in the solid, the available specific impulse is degraded to the maximum attainable corresponding to the reactor solid temperature $T_s$, that is, as $\alpha \rightarrow \infty$, $I_c \rightarrow I_s$.

Another interesting effect to be noted is the very great influence that $\beta$ has on the system at the low values of $\alpha$. In these cases, the fission fraction approaches zero, and the bulk of the heat load in the solid is due to radiation from cavities, both thermal and nuclear. Inasmuch as the reactor size is determined by the power density in the solid, the larger radiative transfer, i.e., larger $\beta$ values, results in larger reactor size and therefore weight. Although in general the smaller values of $\alpha$ yield larger specific impulses, the gains are reduced at the larger values of $\beta$. Thus the power and the reactor and vehicle weights become less sensitive to $\alpha$.

The nuclear characteristics of these systems are shown in Figs. 10 and 11. Fig. 10 gives the average thermal neutron flux $\phi_c$ and the average fuel concentration $N_{FC}$ in the cavity region, as well as the quantity $\alpha N_{FC}$. It may be seen from Eqs. 21 and 26 that the latter is, in fact, the fuel concentration $N_{FS}$ in the solid region of the reactor when $\phi_s = \phi_c$ and $\sigma_f^{(FS)} = \sigma_f^{(FC)}$. The more general relationship is

$$N_{FS} = \alpha N_{FC} \left[ \frac{\sigma_f^{(FC)} \phi_c}{\sigma_f^{(FS)} \phi_s} \right]$$

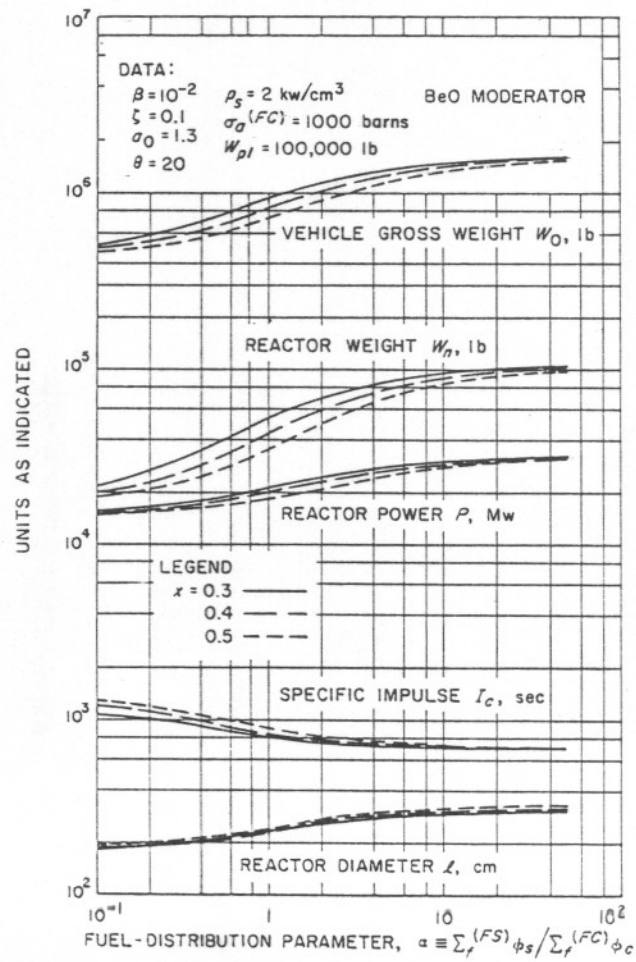


Fig. 12 Influence of cavity-void fraction on vehicle and engine characteristics for Earth-satellite mission

The general dependence of the neutron flux and the fuel concentration $N_{FC}$ on the fuel distribution parameter is evident from Eqs. 18 and 28. The influence on $N_{FC}$ may be seen by rewriting Eq. 18 in the form

$$N_{FC} = \frac{\Sigma_a^{(M)} S_{FM}}{\sigma_a^{(FC)}[S_F(1 - x) + x]}$$

Now $S_F$ is proportional to $\alpha$, therefore at large $\alpha$, $N_{FC}$ varies at least as rapidly as $1/\alpha$. Actually the decrease in fuel concentration is more rapid because, as $\alpha$ increases, so does the reactor size (see Fig. 9), which causes some reduction in $S_{FM}$ (see Fig. 5). The influence of $\alpha$ on the flux is best revealed by the expression

$$\phi_c = \frac{p_s(1 - x)(1 + \alpha_c)}{\epsilon \Sigma_a^{(M)}} \left\{ \frac{I^2[S_F(1 - x) + x]}{S_{FM}[\alpha(1 - x) + x]} \right\}$$

At the large values of $\alpha$, the quantity in the braces behaves essentially as $I^2/S_{FM}$. The most sensitive dependency of $\phi_c$, however, is on $S_{FM}$, since $I_c^2 \rightarrow I_s^2$ at large $\alpha$. Thus $\phi_c \sim 1/S_{FM}$, which still has a rather strong dependency on the reactor size (and therefore $\alpha$) for $x = 0.5$ in the range $200 < l < 500$ cm (see Fig. 5); however, at very large $\alpha$, $S_{FM}$ approaches an asymptote and so does $\phi_c$.

Fig. 11 shows the average fuel concentration $N_F$ and the critical mass $M_F$ as a function of $\alpha$. The asymptotic behavior of $N_F$ at the higher values of $\alpha$ again simply reflects the fact that at the corresponding values of the reactor diameter the fuel concentration function $S_{FM}$ is rapidly approaching its limit $S_{FM}(\infty)$. The interesting behavior of the critical mass curve is explained by the fact that, for the case $x = 0.5$, the reactor sizes for the satellite mission fall in the immediate vicinity of the minimum in the fuel mass curve (see Fig. 6); thus the total fuel inventory is a relatively insensitive function of the fuel distribution parameter.

The influence of the void fraction $x$ on the system characteristics is also of considerable practical importance. Fig. 12 again gives the vehicle and engine characteristics for the satellite mission for the case $\beta = 10^{-2}$, but with variable $x$. The greatest sensitivity to $x$ is seen to occur in the interval $0.2 < \alpha < 10$. Outside this interval $x$ appears to have rather limited influence. Consider first the influence of $x$ for $\alpha < 1$. The essential effect is revealed from the influence of $x$ and $\alpha$ on $\mu$ (see Eq. 5). When $\alpha \ll 1$, $\mu \simeq \alpha(1 - x)(1 - \zeta)/x + \zeta$; thus to zeroth order $\mu \simeq \zeta$ and $f \simeq 0.1$. All systems, regardless of the void fraction, therefore approach the all gas phase configuration, which yields for the specific impulse ratio $\zeta^{-1/2}$, and the resulting system characteristics are essentially the same. At the other extreme $\alpha \gg 1$, $\mu$ and $f$ approach unity, and the system characteristics are again independent of $x$. The only exception is the reactor size. For the large values of $\alpha$, the specific impulse ratio approaches unity, and it may be seen from Eq. 13 that the reactor diameter varies essentially as $(1 - x)^{-1/3}$. Thus, as the void fraction increases, it is to be expected that the reactor size will also increase; this trend is seen in Fig. 12.

Figs. 13 and 14 reveal the influence of the void fraction on the nuclear characteristics. The greatest sensitivity is seen to occur at the smaller values of $\alpha$. The most important of these is the effect on the average fuel concentration $N_F$ and the critical mass. According to Fig. 12, the reactor diameter is not very sensitive to the void fraction, especially for small values of $\alpha$. Thus, if the dependency of $l$ on $x$ is ignored and some value in the range 200 to 300 cm is selected (see Fig. 12), it is immediately apparent from the results shown in Figs. 5 and 6 and Eqs. 18 and 24 that both $N_F$ and $M_F$ increase with increasing void fraction. This behavior is evident in Fig. 14.

The final observation to be made is that the interval $0.2 < \alpha < 10$ will most likely be the range of greatest practical interest for the high thrust systems. In the event that the average thermal fluxes $\phi_s$ and $\phi_c$ are nearly equal in the two fuel-bearing regions of the reactor, then $0.1 < (N_{FC}/N_{FS}) < 5$; thus the concentrations to be maintained in gas phase vary from values comparable to that in the solid down to several per cent of the solid values. This behavior may be seen directly from the fuel concentration curves $N_{FC}$ and $N_{FS}$ in Fig. 10. Now, it may be entirely possible by careful nuclear design to provide some flux peaking in the cavity regions of the reactor. Ratios of $\phi_c/\phi_s \simeq 5$ appear reasonable, and values as large as 10 are not out of question. For the latter situation, $0.01 < (N_{FC}/N_{FS}) < 0.5$; thus it can be seen that, by using flux-peaking techniques, substantial amounts of

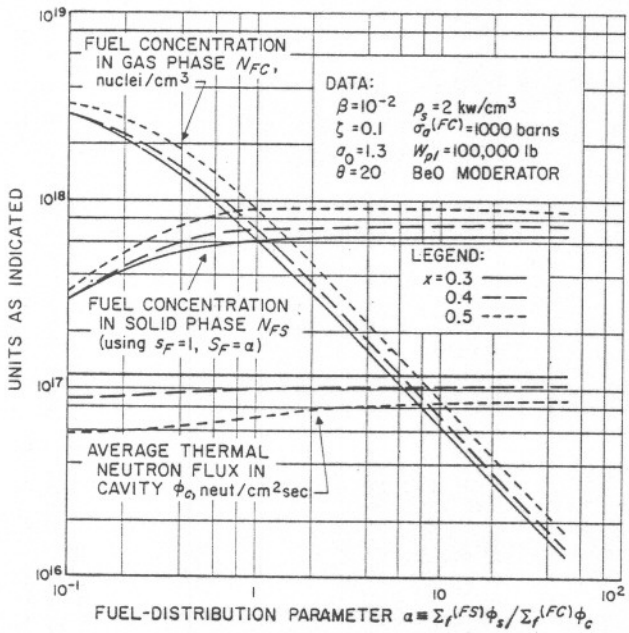


**Fig. 13 Influence of cavity-void fraction on gas and solid phase fuel concentrations and on thermal neutron flux for satellite mission**

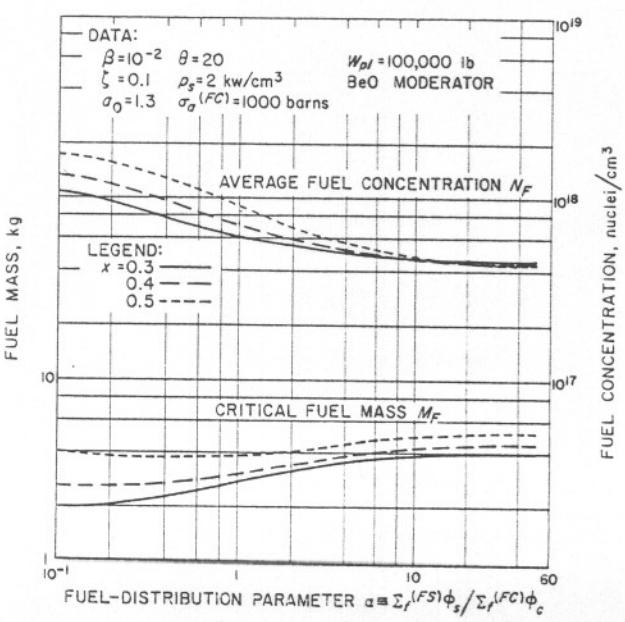


**Fig. 14 Influence of cavity-void fraction on average fuel concentration and critical mass for satellite mission**

gas phase fission heating can be achieved, with gas phase fuel concentrations from $^1/_2$ to $^1/_{100}$ of that carried in the solid regions. Finally, it is of interest to mention the total inventory of fissionable material in the gas phase. Fig. 15 shows the fraction of the critical mass in the gas phase as a function of $\alpha$ for the two values of the flux ratio mentioned above. Clearly, without flux peaking ($\phi_c/\phi_s = 1$), significant increases in specific impulse ($I > 1.5$) can only be achieved by carrying a large fraction of the fuel in gas phase (>60%). With flux peaking, comparable gains in performance can be achieved with as little as 13% of the fuel in gas phase.

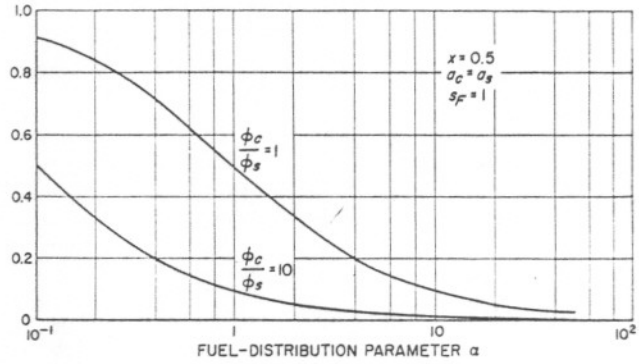


Fig. 15 Fraction of critical mass in gas phase

## Conclusions

The results of this study reveal several interesting characteristics of gaseous propulsion reactors for high thrust application. First, for values of the thermal radiation parameter $\beta$ from $10^{-3}$ to $10^{-1}$, these systems yield specific impulse ratios of from 1.3 to 2.0. It is believed that this range of values for $\beta$ is fairly realistic; thus, it is seen that the incorporation of gaseous fission heating can result in substantial gains in specific impulse over that possible with an all solid fuel propulsion reactor.

The second observation to be made is that the satellite-freighter application offers rather large payload fractions in single-stage vehicles. For the above-mentioned range of $\beta$, this is 0.1 to 0.3.

The third observation is that these vehicles, and therefore payloads, must be necessarily quite large (in the order of 500,000 lb), since the reactor dead weights fall in the range of 10,000 to 100,000 lb.

Finally, it should be pointed out that in order to achieve the specific-impulse ratios noted, the fuel concentration and the fraction of the critical mass in the gas phase must be rather large, if the flux ratio $\phi_c/\phi_s = 1$. For these situations the gas phase fuel concentrations fall in the range of $10^{17}$ to $10^{19}$ nuclei/cm$^3$, and the fraction of the critical mass in the range 0.1 to 0.9. By the introduction of a flux-peaking ratio of, say, $\phi_c/\phi_s = 10$, these values are reduced to $10^{16}$ to $10^{18}$ nuclei/cm$^3$ and 0.02 to 0.5. The importance of the fuel concentration to the question of nuclear fuel economy and gas phase containment is well known (1). It is probable that the difficulty of achieving efficient fuel containment will dictate rather low values of $N_{FC}$. Thus the incorporation of flux-peaking techniques may be essential to a feasibility demonstration.

## References


1 R. V. Meghreblian: Gaseous Fission Reactors for Spacecraft Propulsion. Tech. Report 32-42, Jet Propulsion Lab., Pasadena, Calif., July 6, 1960.

2 J. L. Kerrebrock and R. V. Meghreblian: Vortex Containment for the Gaseous Fission Rocket. *Jour. Aerospace Sci.*, September 1961, vol. 28, pp. 710–724.

3 S. T. Nelson: The Plasma Core Reactor. G.M. 60-7630.2-9, Space Technology Labs. Inc., Los Angeles, Calif., June 22, 1960.

4 H. Weinstein and R. G. Ragsdale: A Coaxial Flow Reactor—a Gaseous Reactor Concept. ARS Preprint 1518-60, presented at ARS 15th Annual Meeting, Washington, D. C., Dec. 5–8, 1960.

5 R. V. Meghreblian: Energy Balance in Plasma Core Reactors for Propulsion. Jet Propulsion Lab. Research Summary 36-11, Nov. 1, 1961, pp. 55–57.

6 R. V. Meghreblian: Thermal Radiation in Gaseous Fission Reactors for Propulsion. Tech. Report 32-139, Jet Propulsion Lab., Pasadena, Calif., July 24, 1961.

7 R. V. Meghreblian and D. K. Holmes: *Reactor Analysis*, pp. 268–302. McGraw-Hill Book Co. Inc., New York, 1960.